COMITATO NAZIONALE PER L'ENERGIA NUCLEARE
Laboratori Nazionali di Frascati

LNF - 68/29
27 Maggio 1968

A. Malecki and P. Picchi: QUASI-ELASTIC ELECTRON SCATTERING ON LIGHT NUCLEI. -

Servizio Documentazione
dei Laboratori Nazionali di Frascati del CNEN
Casella Postale 70 - Frascati (Roma)

Laboratori Nazionali di Frascati del CNEN
Servizio Documentazione

LNF-68/29

Nota Interna: n° 400
27 Maggio 1968

A. Małecki(x) and P. Picchi: QUASI-ELASTIC ELECTRON SCATTERING ON LIGHT NUCLEI. -

(Submitted to Nuovo Cimento for publication).

ABSTRACT. -

Quasi-elastic electron scattering on nucleons bound in light nuclei is considered using the electron-nucleon interaction of Mc Voy and Van Hove. The shell model with the harmonic oscillator potential is assumed to describe the bound nucleons in the initial state. The outgoing nucleon is represented by a plane wave and the probability of the nucleon reabsorption is taken into account by means of a reduction factor. Comparison of the quasi-elastic scattering contribution with the inelastic, experimental cross-section for He^4, C^{12} and O^{16} is presented. The importance of possible effects of short range nucleon-nucleon correlations is discussed.

(x) - On leave of absence from Instytut Fizyki Jadrowej,Krakow, Poland.

1. INTRODUCTION. -

The main features of inelastic electron scattering[x] from nuclei are well known. In a typical experimentally measured inelastic cross-section (see Figs. 1, 2, 4, 5) one can distinguish the following two parts:

a) at small energy transfers a number of peaks corresponding to the excitation of discrete nuclear levels are seen;
b) at large energy transfers the cross-section follows an almost smooth curve in which only little structure is apparent.

The large energy transfer part of the spectrum is referred to as the quasi-elastic scattering. It corresponds roughly to direct collisions with the individual, quasi-free nucleons in the nucleus. For a fixed incident electron energy ε and scattering angle θ, this part of the cross-section looks like a big bump on the experimental curve (see Figs. 1, 2).

The present paper deals with the quasi-elastic scattering. There are two reasons of our interest. Above all, the quasi-free scattering is expected to be the dominant inelastic process, especially at high energies. It would therefore be desirable to know fairly well the principal contribution which almost exhausts the inelastic sum rule, not only in the electron scattering, but in any electromagnetic process on nuclear target. It has also been suggested[1] that the tail of the quasi elastic bump (very large energy transfers) should be very sensitive to the nucleon-nucleon correlations. In order to obtain a valuable information about nuclear structure, however, one first has to understand much better the quasi-elastic scattering itself.

From any quasi-free scattering calculations we would expect the following features:

1) the quasi-free cross-section should not exceed anywhere the experimental cross-section as the quasi-elastic events (i. e. events where the struck nucleon escaped the nucleus without secondary interaction) represent only a subclass of the inelastic events. Therefore a comparison of the quasi-elastic cross-section with the experimental one can only yield information about the relative importance of the quasi-free contribution;

(x) - We discuss the non-coincidence experiments where one observes only the final electron. Coincidence experiments involving detection of final nuclear products together with the final electron, like the recent experiments of Amaldi et al.[11, 12], on the (e, e', p) reaction, are still scarce. Their number should, however, increase in the near future with the increasing number of the high duty cycle accelerators now under construction.

2) the quasi-free cross-section should be fairly small in the region of small energy transfers where the scattering to discrete nuclear levels presumably dominates.

The existing quasi-elastic scattering calculations[2, 3] were based on a Fermi gas model and compared with the experiments on ^{12}C. They fit very well the large energy transfer side of the experimental bump (see, especially the fits of Czyż[2]), but at small energy transfers these calculations have a drawback, giving numbers which even exceed the experimental data.

We use, for the description of the nuclear ground state, a more appropriate model for light nuclei, namely the shell model with the harmonic oscillator potential. The ejected nucleon is represented by a plane wave. The last assumption is justified as we take into account the distortion effect in the final state by means of a reduction factor.

The general formalism is presented in Section II. The numerical results and a comparison with the experimental data for ^4He, ^{12}C and ^{16}O is given in Section III.

II. GENERAL FORMALISM. -

Let us consider the scattering of an electron with incident energy $\mathcal{E}$ (which is sufficiently high to neglect the electron rest mass) through an angle θ to a final state with energy $\mathcal{E}'$, while the nucleus makes a transition from the ground state $|i\rangle$ to the state $|f\rangle$. The cross section for this process (we assume that one observes only the final electron) is given, in the first Born approximation, by the following[4] formula(*):

$$\frac{d^2\sigma}{d\mathcal{E}'\,d\Omega'} = \frac{e^4\cos^2\theta/2}{4\,\mathcal{E}^2\sin^4\theta/2}\,\overline{\sum_{|i\rangle}}\sum_{|f\rangle}\delta(\omega - E_f + E_i)\left\{\frac{q_\alpha^4}{q^4}\,Q^*_{fi}\,Q_{fi} + \right.$$

$$\left. + (\tan^2\theta/2 - q_\alpha^2/2q^2)\left[\vec{J}^*_{fi}\cdot\vec{J}_{fi} - \frac{1}{q^2}(\vec{J}^*_{fi}\cdot\vec{q})(\vec{J}_{fi}\cdot\vec{q})\right]\right\}_{LAB} \tag{1}$$

where

$$\omega = \mathcal{E} - \mathcal{E}',\quad q_\alpha^2 = \omega^2 - q^2;$$

(*) - We use a metric such that $a_\mu = (a_0, \vec{a})$ and $a_\mu\, b_\mu = a_0\, b_0 - \vec{a}\cdot\vec{b}$. The magnitude of the three vector is $a = |\vec{a}|$. We also use units $c = \hbar = 1$, $e^2 = 1/137$.

q being the three momentum transfer to the nucleus. $Q_{fi} = \langle f | Q(\vec{q}) | i \rangle$, $J_{fi} = \langle f | \vec{J}(\vec{q}) | i \rangle$ are the matrix elements between the ground and excited states of the charge and current operators of the target nucleus, respectively. In Eq. (1) all the quantities are to be taken in the laboratory frame.

Eq. (1) gives the most general form of the cross-section for the non-coincidence experiment. In order to perform the calculations we have to make some assumptions about the nuclear charge and current operators. We neglect exchange currents and assume the charge and current operator of the nucleus to be the sum of the operators for the individual nucleons. Following Mc Voy and Van Hove[5] we use the non relativistic form of the charge and current operators including terms to the order $1/M^2$ (M-nucleon mass):

$$Q(\vec{q}) = f(q_\mu^2) \sum_{j=1}^{A} \left\{ \left[e_j - \frac{q_\mu^2}{8M^2} (e_j - 2\mu_j) \right] e^{i\vec{q}\cdot\vec{r}_j} \right\}$$

(2)

$$\vec{J}(\vec{q}) = f(q_\mu^2) \sum_{j=1}^{A} \left\{ \frac{e_j}{2M} (\vec{p}_j e^{i\vec{q}\cdot\vec{r}_j} + e^{i\vec{q}\cdot\vec{r}_j} \vec{p}_j) + \frac{\mu_j}{2M} i (\vec{\sigma}_j \times \vec{q}) e^{i\vec{q}\cdot\vec{r}_j} \right\}$$

where one sums over all the nucleons in the target nucleus and e_j, μ_j are the charge and total magnetic moment (in the nuclear magnetons) for the j-th nucleon; $\vec{r}_j$, $\vec{p}_j$, $1/2\ \vec{\sigma}_j$ are its position, momentum and spin operators, respectively.

In Eq. (2) we have used an approximation concerning the nucleon electromagnetic form factor, namely it was assumed the same form for the Dirac and Pauli form factors:

$$F_{1p}(q_\mu^2) = F_{2p}(q_\mu^2) = F_{2n}(q_\mu^2) = f(q_\mu^2), \qquad \text{while} \qquad F_{1n}(q_\mu^2) = 0 .$$

The charge and current operators (2) when applied to Eq. (1) result in the following formula for the cross-section:

$$\frac{d^2\sigma}{d\varepsilon' d\Omega'} = \frac{e^4 \cos^2\theta/2}{4\varepsilon^2 \sin^4\theta/2} f^2(q_\mu^2) \left\{ \frac{q_\mu^4}{q^4} \left[1 + (2\mu_p - 1) \frac{q_\mu^2}{4M^2} \right] R_1(q,\omega) + \right.$$

(3)

$$\left. + (\tan^2\frac{\theta}{2} - \frac{1}{2} q_\mu^2/q^2) \left[R_2(q,\omega) + (\mu_p^2 + \mu_n^2) \frac{q^2}{2M^2} R_1(q,\omega) \right] \right\}$$

$R_{1,2}(q,\omega)$ are some functions of the momentum and energy transfer to the nucleus. We call them the response functions. $R_1(q,\omega)$ describes

interaction with the nucleon charge and spin-part of the current, whereas $R_2(q,\omega)$ comes from the interaction with the nucleon convection current. The formula (3) is correct for nuclei with the same number of protons and neutrons in both spin states.

For our quasi-elastic calculations the following model was assumed. We use[6] the shell model for the description of the ground state of the nucleus. The ejected nucleon is represented by a plane wave. In fact its wave is a distorted one, but one can still work with plane waves, as we will take into account the probability of the nucleon reabsorption. We shall do this by means of the reduction factor $D(\omega)$ defined as the probability that the ejected nucleon will not share its energy with other nucleons in the nucleus. Under these assumptions the response function are given by the following expressions:

$$(4a)\qquad R_1 = \frac{1}{2}\sum_{|a\rangle} N_a D_a \int d^3p\, W_a(\vec{p})\,\delta\left(\omega - \frac{(\vec{p}+\vec{q})^2}{2M} - \frac{p^2}{2M(A-1)} - S_a\right)$$

$$(4b)\qquad R_2 = \frac{1}{2}\sum_{|a\rangle} N_a D_a \int d^3p \left[p^2 - \frac{(\vec{p}\cdot\vec{q})^2}{q^2}\right] W_a(\vec{p})\,\delta\left(\omega - \frac{(\vec{p}+\vec{q})^2}{2M} - \frac{p^2}{2M(A-1)} - S_a\right)$$

where one sums over the single-particle orbital states occupied by nucleons in the ground state. S_a and N_a are the nucleon separation energy and number of nucleons in the state $|a\rangle$ while $W_a(p)$ is the nucleon momentum distribution in this state. In Eqs. (4) we have taken into account the recoil energy of the residual nucleus (A is the mass number of the target).

We choose the shell model potential to be the harmonic oscillator potential well.

For nuclei with filled s-shell ($N_o=4$) and Z-2 protons and neutrons in p-shell ($N_1=2(Z-2)$) we get from (4):

$$(5a)\qquad R_1 = \frac{M}{\sqrt{\pi}\,\alpha q}\sum_{l=0,1}\frac{2^l N_l D_l}{2l+1}\, e^{-(\Omega_1+2)t_1}\left\{\left[1+l(\Omega_1+2)t_1\right]\sinh\left(2\sqrt{\Omega_1+1}\,t_1\right) - 2l\sqrt{\Omega_1+1}\,t_1\cosh\left(2\sqrt{\Omega_1+1}\,t_1\right)\right\}$$

$$(5b)\qquad R_2 = \frac{\alpha}{2\sqrt{\pi}\,Mq}\sum_{l=0,1}\frac{2^l N_l D_l}{(2l+1)t_1}\, e^{-(\Omega_1+2)t_1}\left\{2\sqrt{\Omega_1+1}\,t_1\left[2l+1+l(\Omega_1+2)t_1\right]\cosh\left(2\sqrt{\Omega_1+1}\,t_1\right) - \left[4l(\Omega_1+1)t_1^2+l(\Omega_1+2)t_1+2l+1\right]\sinh\left(2\sqrt{\Omega_1+1}\,t_1\right)\right\}$$

where

$$(5c)\qquad \Omega_1 = \frac{A}{A-1}\left(\omega - S_1 - \frac{q^2}{2M}\right)\frac{2M}{q^2}\quad , \qquad t_1 = \left(\frac{A-1}{A}\,\frac{q}{\alpha_1}\right)^2$$

α_1 being the oscillator potential parameter (the oscillator spacing equals α_1^2/M) for the 1-shell.

The reduction factor[7] is given by the integral over the nucleus of the probability that the nucleon struck at the point $\vec{r}$ will leave the nucleus without secondary interaction, in the direction given by a versor $\hat{n}$:

$$(6)\qquad D_1(\sigma) = \frac{1}{N_1}\int d^3 r\, \varrho_1(\vec{r})\exp\left\{-\sigma\int_{\vec{r}}^{\infty} ds\,(\vec{r},\hat{n})\left[\sum_{k=0,1}\varrho_k - \frac{\varrho_1}{N_1}\right]\right\}$$

where ϱ_1 is the nucleon density for the 1-shell, σ is the effective nucleon--nucleon cross-section. As we make an average over the nuclear volume, the reduction factor is, in fact, independent of the direction $\hat{n}$. It depends only on σ, which is a certain function of the kinetic energy of outgoing nucleon, and hence a function of energy transfer to the nucleus. Using, consistently, in (6) the nucleon densities, as determined by the oscillator potential well, we get for the 1p-shell nuclei the following formulas for the reduction factors, corresponding to the nucleon ejected from s - and p-shell:

$$(7)\qquad D_s(\omega) = \int_0^1 du\exp\left\{-\sigma(\omega)\frac{\alpha_s^2}{6\pi}u\left[9+2(Z-2)\frac{\alpha_p^2}{\alpha_s^2}u^{\frac{\alpha_p^2}{\alpha_s^2}-1}\cdot\left(1-2\frac{\alpha_p^2}{\alpha_s^2}\ln u\right)\right]\right\}$$

$$(8)\qquad D_p(\omega) = \frac{1}{3}\int_0^1 du\,(1-2\ln u)\exp\left\{-\sigma(\omega)\frac{\alpha_p^2}{6\pi}u\left[12\frac{\alpha_s^2}{\alpha_p^2}u^{\frac{\alpha_s^2}{\alpha_p^2}-1}+(2Z-5)(1-2\ln u)\right]\right\}$$

where the oscillator parameters for the two shells were assumed to be different.

The reduction factors resulting from (7) and (8) are presented in Fig. 3, for the C^{12} target case, as the functions of σ. It is interesting to compare our values with those of Jacob and Maris[8], which have been obtained, in a different way, at $\sigma = 29$ mb. Our curves denoted "2" give (for

explanation see the next chapter) nearly the same numbers, as in ref. (8) for both shells.

In order to evaluate with the aid of (3), (5), (7) and (8) the quasi-elastic scattering cross-section as the function of energy transfer, we have to know the dependence $\sigma = \sigma(\omega)$. We assumed that the effective nucleon-nucleon cross-section $\sigma(\omega)$, which enters in the reduction factor calculations, is the A-th part of the neutron or proton total reaction cross-section for the target nucleus, respectively, taken at the mean kinetic energy of the outgoing nucleon. This mean energy equals (see Eq. (4)) $\bar{T} = \omega - S - \langle p^2 \rangle / 2(A-1)M$; $\langle p^2 \rangle$ being the mean square nucleon momentum in a given shell. This is very simple, but seems also to be quite a reasonable assumption. Thus the only secondary interaction which we admit for the outgoing nucleon is the elastic scattering in the nuclear optical potential. The events, which would "spoil" the quasi-elastic contribution, i.e. events where the ejected nucleon shared its energy with other nucleons in the nucleus, are, however, excluded from the calculations.

Before closing this chapter we should like to mention certain limitation for our calculations. It was explicitly assumed in our treatment that the electron interacts with only one nucleon in the shell model potential well, but does not cause any collective motions or excitations of various groups of nucleons. This means that the momentum transferred through the intermediate virtual photon to the nucleus should be sufficiently high, as the probability of the collective, i.e. non quasi-elastic type excitations would then be highly reduced. This probability is given roughly by the square of the elastic form factor[9] (normalized to unity at $q = 0$) of the target $F^2(q)$ and, e.g. for the C^{12} target is negligible[10] for momentum transfers $\gtrsim$ 250-300 MeV.

From this discussion the conclusion follows: if the kinematical conditions of the experiment, e.g. electron energy $\mathcal{E}$ and scattering angle θ are so chosen that the corresponding momentum transfers are sufficiently large, the quasi-elastic scattering formulas (3) and (5) can be used with confidence; on the other hand, at small momentum transfers, the factor $1 - F^2(q)$ can be treated as an estimate of the probability that one is really dealing with the quasi-elastic scattering. Using $1 - F^2(q)$ as an additional reduction factor we hope to be able to describe the average properties of the quasi-elastic scattering contribution. This is confirmed by the analysis presented in Fig. 2, where the two sets of the quasi-elastic scattering curves with and without the factor $1 - F^2(q)$ respectively are compared with experimental data (for more details see the next chapter). The curves obtained with the extra reduction factor encourage us to use it with more confidence.

III. NUMERICAL RESULTS AND DISCUSSION. -

The results of our quasi-elastic scattering calculations for C^{12}, O^{16} and He^4 are presented and compared with experimental data in Figs. 1-2, 4 and 5, respectively. The curves for C^{12} and He^4 are calculated at constant incident electron energy $\mathcal{E}$ and constant scattering angle θ, while that for O^{16} at constant $\mathcal{E}$ and constant three-momentum transfer q. We have used the nucleon separation energies for the s - and p-shell as determined through (e, e'p)[11] and (p, 2p)[13] reactions. The same separation energies for protons and for neutrons were assumed. This is, however, an inessential deficiency, since the proton separation energies are only known with an uncertainty of a few MeV. In the case of C^{12} and O^{16} the two sets of the oscillator potential parameters have been tried. The curves denoted "1" have been obtained with the same oscillator parameter for both shells $\alpha_s = \alpha_p = \alpha$ while the curves "2" were calculated with the different parameters[14] for the s - and p-shell: $\alpha_s \neq \alpha_p$. Both the sets of parameters give the correct root-mean-square radius of the target; moreover; in the case of curves "2" the same dimension of the s-shell as that of the He^4 nucleus[18] was assumed.

In our calculations the following phenomenological representation of the nucleon electromagnetic form factor[15] was assumed:

$$f(q_\mu^2) = \left(1 - \frac{a^2}{12}\, q_\mu^2\right)^{-2} \tag{9}$$

with the nucleon r.m.s. radius $a = 0.8 \cdot 10^{-13}$ cm.

Let us discuss Figs. 1-5 in more detail. In Fig. 1 are presented our results for C^{12}, at incident electron energy $\mathcal{E} = 198$ MeV and scattering angle $\theta = 135^o$. The experimental data in Fig. 1 are those of Bounin and Bishop[16], whereas the curve denoted "L" comes from recent calculations of Løvseth[3]. The curve "1" has been obtained with the same oscillator parameter for both shells - $\alpha = 120.5$ MeV[17], while in the case of curve "2" we have used the different oscillator parameters, namely $\alpha_s = 148.3$ MeV[18], $\alpha_p = 114.8$ MeV. Both curves are calculated with the nucleon separation energies: $S_s = 34$ MeV and $S_p = 14$ MeV, for the s - and p-shell, respectively. The reduction factors for C^{12} are presented in Fig. 3. The curves denoted "1" and "2", correspond to the same sets of the oscillator parameters as above, respectively. In order to obtain with the aid of these curves, the reduction factors as a function of the energy transfer ω, we applied the method described in chapter II, making use of the neutron and proton total reaction cross-sections for carbon. The latter have been taken from ref. (19). Since momentum transfers in the experiment described in Fig. 1 are sufficiently large (ranging from 330 MeV to 230 MeV), the extra reduction factor, which we mention at the end of Chapter II, is not important in this case (it gives at most the 5% change[10] for the large

ωs tail of the quasi-elastic bump), and was dropped in our calculations.

This factor however is very important in the case of the experiment, presented in Fig. 2. The experiment was performed on C^{12}, by Leiss and Taylor[2], at incident electron energy $\mathcal{E} = 80.9$ MeV and scattering angle $\theta = 135^{o}$. Momentum transfers are now rather small, ranging from 135 MeV to 100 MeV, and the introduction of the extra reduction factor $1 - F^2(q)$ much improves the quasi-elastic scattering curves. The curves "1" and "2" in Fig. 2 have been obtained with the aid of Eqs. (3), (5) and Fig. 3 using the same parameters for C^{12}, respectively, as given earlier.

The results of our quasi-elastic scattering calculations for O^{16}, at incident electron energy $\mathcal{E} = 140$ MeV and fixed momentum transfer $q = 190$ MeV, are presented in Fig. 4, where they are also compared with the experimental data of Bishop et al.[20]. The curve "1" has been obtained with the oscillator parameters $\alpha_s = \alpha_p = 111.9$ MeV[17], while in the case of curve "2" we have used $\alpha_s = 148.3$ MeV[18] and $\alpha_p = 107.3$ MeV. For both curves the nucleon separation energies $S_s = 38$ MeV, $S_p = 16$ MeV are assumed. As the reduction factor curves for O^{16} are very similar to those for C^{12} they are not presented. Related to C^{12} the reduction factors for O^{16} are a little smaller, e.g. at $\sigma = 29$ mb we get the following values of the reduction factors for C^{12} and O^{16}, respectively (we give numbers resulting from the curves "2" calculated with the different oscillator parameters): 0.44 and 0.38 for s-shell, and 0.62, 0.58 for p-shell. The nucleon reaction cross-section on O^{16}, which are necessary in order to obtain the reduction factors as a function of energy transfer, were deduced from the cross-sections for carbon[19] according to an assumed $A^{2/3}$ law[19, 21]. As in the experiment on O^{16} the momentum transfer is fixed, the extra reduction factor is independent of energy transfer. We have not taken it into account. It would make the curves in Fig. 4 about 10%[10] lower.

Finally, in Fig. 5 we have presented the quasi-elastic scattering curves for the He^4 target, at incident electron energy $\mathcal{E} = 299$ MeV and scattering angle $\theta = 54.6^{o}$. Experimental data come from the recent work of Frosch et al.[22]. The theoretical curves (with and without the extra reduction factor $1 - F^2(q)$ have been calculated with the oscillator parameter $\alpha = 148.3$ MeV[18] and the nucleon separation energy $S = 20$ MeV. In this case the factor $1 - F^2(q)$ equals about 0.8[10], while the reduction factor given by Eq. (7) was assumed to be 1.0. This value is justified for sufficiently small ($\omega \leqslant 46$ MeV) energy transfers, since the reaction cross-section on He^4 vanishes[23] for the nucleon energies below 20 MeV. At larger ω's one has, however, to take into account the effect of the reduction factor.

Before comparing the results of the present calculations with experimental data we would like to stress the two features concerning the quasi-elastic contribution which were already mentioned in the introduction.

Our quasi-elastic scattering curves exhibit both these features: they do not exceed almost anywhere the experimental cross-sections and, in the region of small energy transfers, the quasi-elastic contribution is fairly small.

A few comments are relevant here.

1) Our calculations confirm the dominance of the quasi-elastic contribution, especially at large energy transfers. The inelastic sum rule calculated when considering only the quasi-elastic events could represent an instructive estimate from below for the integral contribution of inelastic processes. The "true" inelastic sum rule, including contributions from all possible inelastic events, would be about 20-30% bigger.

2) Our quasi-elastic scattering curves in Figs. 2 and 4 have a certain structure which is also apparent in the experimental data. We mean about a small hump appearing at an energy transfer of 40 MeV. The effect has not been seen in the calculations[2, 3] based on the Fermi gas model and could be easily attributed to the shell structure of the nucleus. In that region of energy transfers the quasi-elastic scattering on the s-shell nucleons begins to be important and to compete with the p-shell contribution. In the experiment presented in Fig. 1 this effect is no more evident, because in this case the quasi-elastic contribution from the nucleons in s-shell is given by a very flat curve.

3) The difference between the curves "1" and "2", obtained with the same and different oscillator potential parameters for s- and p-shells, respectively, is rather small (see Figs. 1, 2 and 4).

4) Our calculations show the existence of two regions of energy transfers where the experimental cross-section significantly exceeds the quasi-elastic one. One can hope to obtain an information about nucleon-nucleon correlations from these regions.

The first region corresponds to small and medium energy transfers: 10-70 MeV in Fig. 1, 10-32 MeV in Fig. 2, 10-40 MeV in Fig. 4. The difference between the quasi-elastic curve and the experimental cross-section is due to a minimum in the reduction factor curves which appears at these energy transfers. The minimum is a reflection of the broad peak in the nucleon reaction cross-section on nuclei which falls in the region 10-50 MeV[19,21]. This peak can be accounted for either by the large value of the elementary nucleon-nucleon cross-section in this region of nucleon energies or by the importance of internucleon correlations (of the long or short range) in the nucleus. In conclusion, it seems that in the region of small and medium energy transfers it would be rather difficult to extract a well defined information about nuclear structure, since the experimental numbers are produced by many effects of different physical origin.

The second region where the experimental cross-section significantly exceeds the quasi-elastic curve occurs at very large energy transfers, as

it is seen in Fig. 1 and was already demonstrated by the previous calculations[1,2].

Czyż and Gotfried[1] have argued that quasi-elastic scattering should be negligible for

(10) $$\omega > \omega_h = q^2/2M + qk_F/M + q/MR$$

where k_F is the Fermi momentum and R is the radius of the nucleus. Therefore the scattering at very large energy transfers is mainly due to nucleon correlations and hopefully one can obtain some nontrivial information about nuclear structure from this region. As this is a very important and challenging problem we should like, before concluding this paper, to discuss the kinematical conditions of the experiment at which the effect of internucleon correlations would best be visible. Comparison of Figs. 1 and 4 shows that the exact distinction between the quasi-elastic contribution and the experimental cross-section is more feasible in the experiment performed at constant electron energy $\mathcal{E}$ and constant scattering angle θ, because of the characteristic form of the quasi-elastic scattering curve in this case. In the constant $\mathcal{E}$, θ experiment the momentum transfer varies with ω and reaches its minimum value $q = q_{min}$ at energy transfer

(11) $$\omega = \omega_{min} = 2\mathcal{E}\sin^2\theta/2$$

The momentum transfers in the experiment should be sufficiently large in order to detect better short range two-nucleon correlations, as e.g. hard-core effects, which presumably dominate at high ω's; moreover, at large q, the quasi-elastic formulas (3) and (5) are more reliable. For these reasons (in the case C^{12} and O^{16}) we impose the condition $q \gtrsim 300$ MeV. In this region of momentum transfer we are still safely far from the maximum q at which the $1/M^2$ approximation used in (2) is useful and which has been estimated to be[5] about 500 MeV. It is reasonable to assume that suitable values of $\mathcal{E}$ and θ for the experiment are given by the condition: $\omega_{min} = \omega_h$. This condition gives:

(12a) $$\mathcal{E} = \frac{1}{2\omega_h}\,(q_{min}^2 + \omega_h^2)$$

(12b) $$\theta = 2 \arcsin \sqrt{\frac{\omega_h}{2\mathcal{E}}}$$

Putting $q_{min} = 300$ MeV and using $k_F = 1.48\,f^{-1}$[24], $R = 3.12f$ (radius of the equivalent uniform charge distribution for carbon[10]) we obtain from (10) and (12): $\mathcal{E} \approx 360$ MeV and $\theta \approx 56^\circ$. For these values of $\mathcal{E}$ and θ the region where scattering can be ascribed to dynamical correlations in the nuclear

ground state begins at about 160 MeV. It is somewhat above the meson production threshold but the particle production effects are still negligible[25] at these energy transfers.

Concluding this paper we should like to stress that a lot of interesting work on the subject, both experimental and theoretical, remains to be done. It would be very desirable to have more complete measurements of the inelastic electron scattering cross-section, especially for large momentum and energy transfers. It is also necessary to dispose of a reliable method which would take into account the dynamical nucleon-nucleon correlation corrections to the basic, quasi-elastic scattering contribution.

REFERENCES. -

(1) - W. Czyż and K. Gotfried, Ann. Phys. 21, 47 (1963).
(2) - W. Czyż, Phys. Rev. 131, 2141 (1963).
(3) - J. Løvseth, CERN Report TH. 861 (1967).
(4) - A. Małecki, Laboratori Nazionali di Frascati, LNF-67/51 (1967).
(5) - K. W. Mc Voy and L. Van Hove, Phys. Rev. 125, 1034 (1962).
(6) - V. Devanathan, Ann. Phys. 43, 74 (1967).
(7) - T. Ericson, F. Selleri and R. Van de Walle, Nuclear Phys. 36, 353 (1962).
(8) - G. Jacob and Th. A. J. Maris, Nuclear Phys. 31, 152 (1962).
(9) - W. Czyż, L. Leśniak and A. Małecki, Ann. Phys. 42, 97 (1967).
(10) - R. Herman and R. Hofstadter, High Energy Electron Scattering Tables, Stanford Univ. Press, Stanford (1960).
(11) - U. Amaldi Jr., G. Campos Venuti, G. Cortellessa, G. Fronterotta, A. Reale, P. Salvadori and P. Hillman, Phys. Rev. Letters 13, 341 (1964).
(12) - U. Amaldi Jr., G. Campos Venuti, G. Cortellessa, E. De Sanctis, S. Frullani, R. Lombard and P. Salvadori, Phys. Letters 25B, 24 (1967).
(13) - G. Jacob and Th. A. J. Maris, Revs. Modern Phys. 38, 121 (1966).
(14) - C. Ciofi degli Atti, Nuclear Phys. A106, 215 (1968).
(15) - R. Hofstadter, Ann. Rev. Nuclear Sci. 7, 231 (1957).
(16) - P. Bounin and G. R. Bishop, J. Physique 24, 974 (1963).
(17) - U. Meyer-Berkhout, K. W. Ford and A. E. S. Green, Ann. Phys. 8, 119 (1959).
(18) - H. Frank, D. Haas and R. Prange, Phys. Letters 19, 391 (1965) and 19, 719 (1965).
(19) - R. E. Pollock and G. Schrank, Phys. Rev. 140B, 575 (1965).
(20) - G. R. Bishop, D. B. Isabelle and C. Betourne, Nuclear Phys. 54, 97 (1964).
(21) - M. Q. Makino, C. N. Waddel and R. M. Eisberg, Nuclear Phys. 50, 145 (1964).

(22) - R. F. Frosch, R. E. Rand, H. Crannell, J. S. Mc Carthy, L. R. Suelzle and M. R. Yearian, Nuclear Phys. A110, 657 (1968).
(23) - M. Arnold, P. E. Hodgson, D. F. Shaw and D. M. Skyrme, Nuclear Phys. 19, 500 (1960).
(24) - M. A. Preston, Physics of the nucleus (Addison Wesley Publishing Company, 1962).
(25) - W. Czyż and J. D. Walecka, Nuclear Phys. 51, 312 (1964).

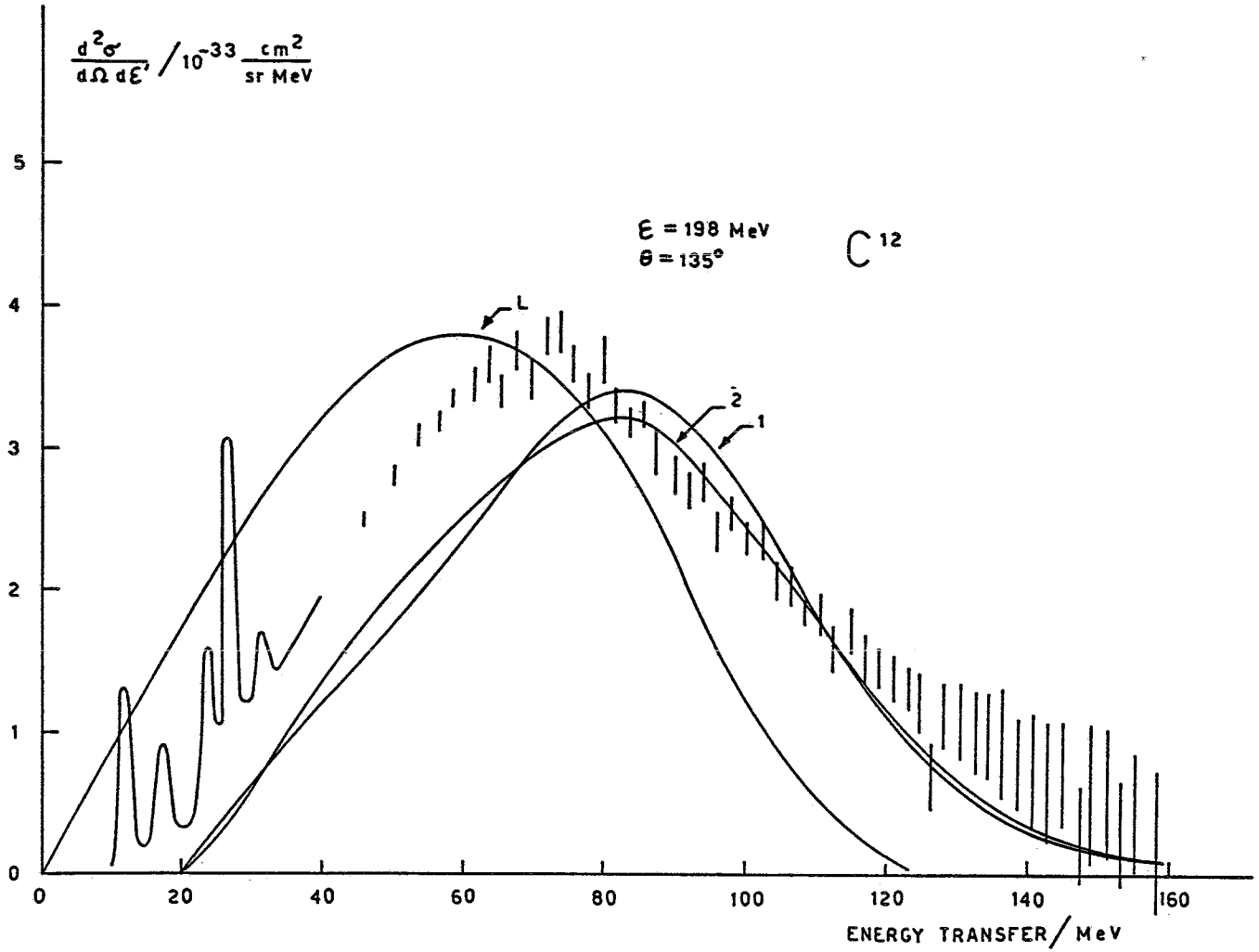

FIG. 1 - Comparison of the experimental inelastic cross-section on C^{12} (large momentum transfers experiment) with the calculated quasi-elastic contribution (curves "1", "$\overline{2}$" and "4"). For more details see text.

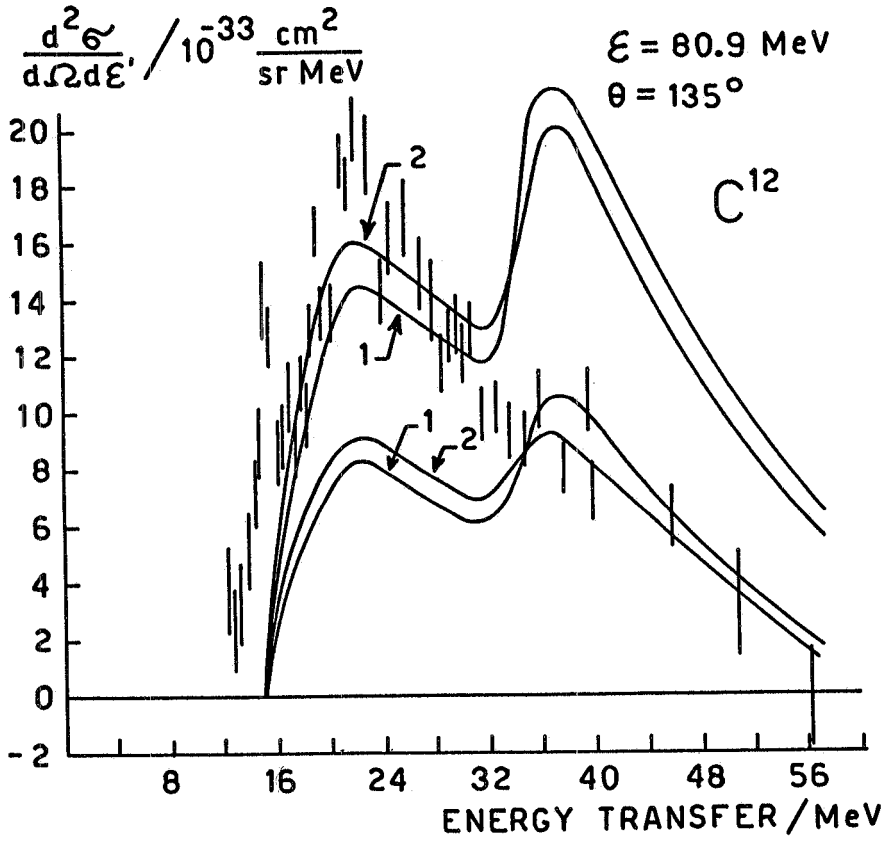

FIG. 2 - Comparison of the experimental inelastic cross-section on C^{12} (small momentum transfers experiment) with the calculated quasi-elastic contribution (curves "1" and "2"). The lower curves are obtained with the extra reduction factor.

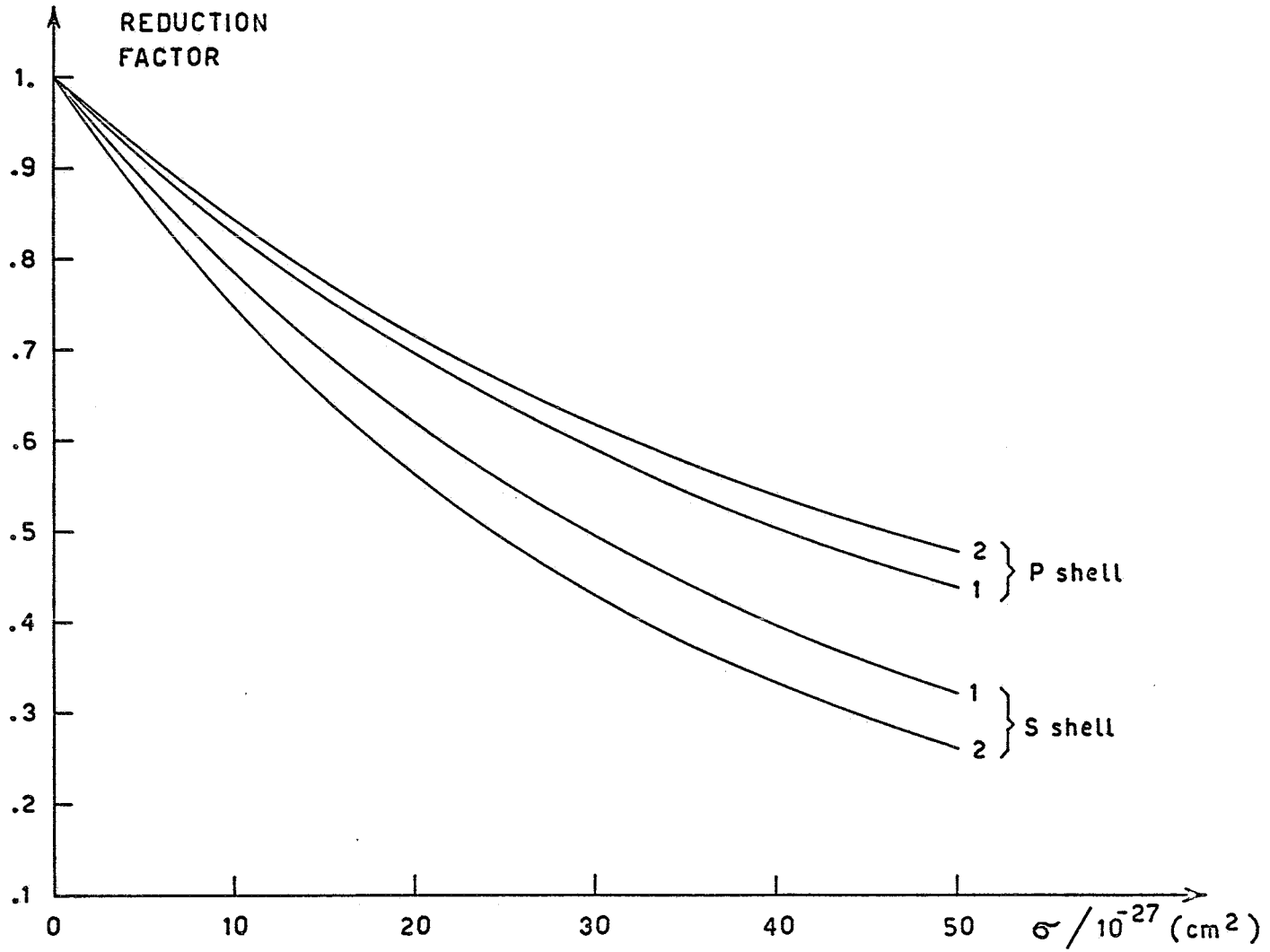

FIG. 3 - Reduction factors for C^{12} as the function of the effective nucleon-nucleon cross-section.

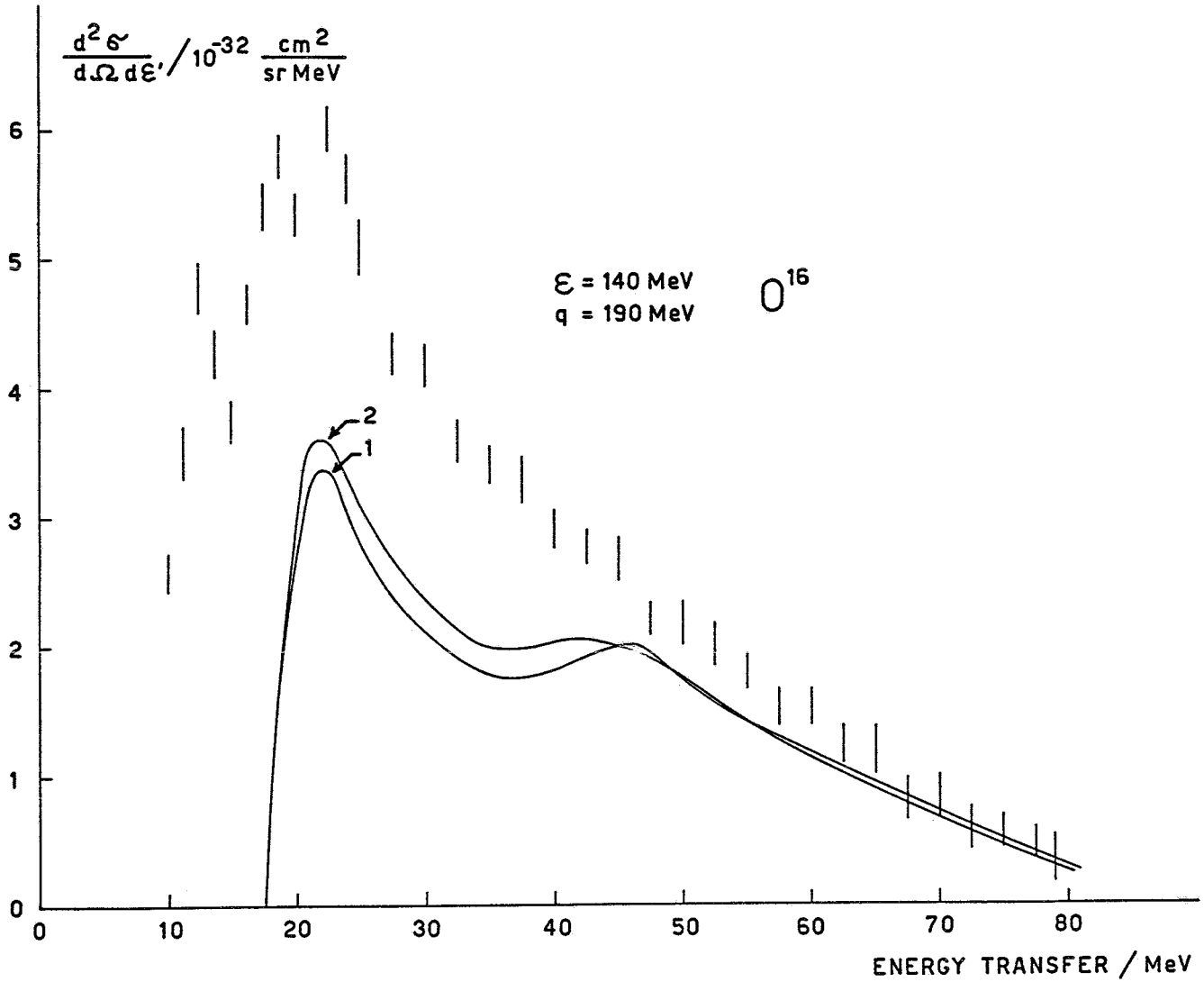

FIG. 4 - Comparison of the experimental inelastic cross-section on O^{16} with the calculated quasi-elastic contribution (curves "1" and "2" - see text).

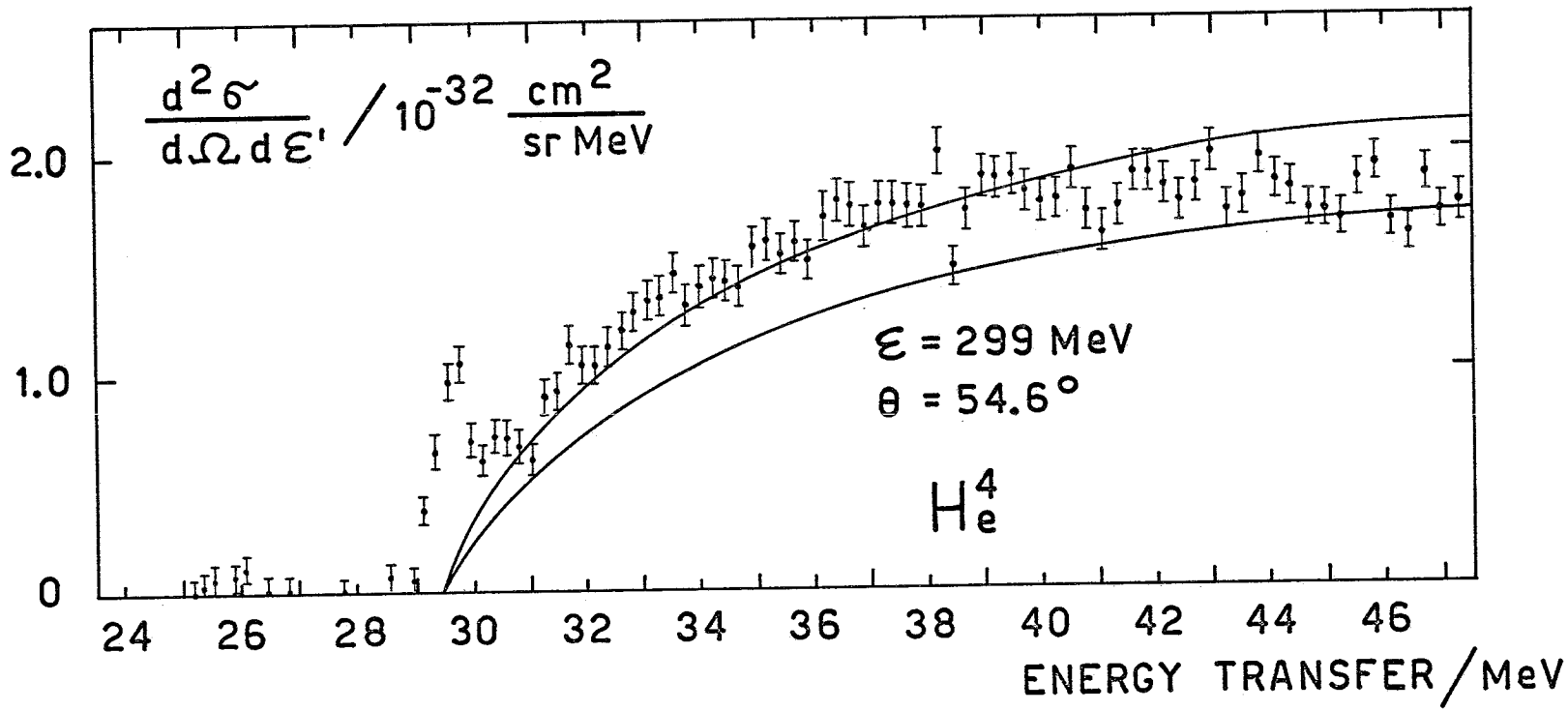

FIG. 5 - Comparison of the experimental inelastic cross-section on He^4 with the quasi-elastic contribution. The lower curve is obtained with the extra reduction factor.